THE ROLE OF ACID SPHINGOMYELINASE IN AUTOPHAGY

Matthew Jose Justice

Submitted to the faculty of the University Graduate School
in partial fulfillment of the requirements
for the degree
Master of Science
in the Department of Biochemistry and Molecular Biology,
Indiana University

December 2013

Accepted by the Graduate Faculty, Indiana University, in partial fulfillment of the requirements for the degree of Master of Science.

Irina Petrache, M.D., Chair

Janice S. Blum, Ph.D.

Master's Thesis
Committee

Ronald C. Wek, Ph.D.

Acknowledgments

First and foremost, I would like to graciously thank my mentor, Irina Petrache. I am indebted to her for support, guidance, patience, wisdom, showing me how to be patient, and making this degree is possible. I would like to give thanks to Janice Blum and Ronald Wek for agreeing to serve as committee members and for providing insight and stimulating questions while doing so. I would like to extend my gratitude to Kelly Schweitzer for her teaching, understanding, and willingness to help me succeed. I would like to show appreciation to Daniela Petrusca, Christophe Poirier, and Mary Van de Mark, for help with various assays and support in the lab, but most of all, for being friends and not just colleagues. I would also like to give thanks to my former mentor, Horia Petrache for giving direction and answering “the tough questions”. My three daughters, Savana, Karianne, and Eliana have provided sanity at the end of the day through smiles and tea parties, I am grateful for them. Words cannot truly express the full depth of my appreciation and gratitude for my wife, LaDonna. Without her, I am nothing.

Funding Source: RO1HL077328 (IP)

Matthew Jose Justice

THE ROLE OF ACID SPHINGOMYELINASE IN AUTOPHAGY

Autophagy is a conserved cellular process that involves sequestration and degradation of cytosolic contents. The cell can engulf autophagic cargo (lipids, long-lived proteins, protein aggregates, and pathogens) through a double bound membrane called an autophagosome that fuses with a lysosome where hydrolases then degrade these contents. This process is one of the main defenses against starvation and is imperative for newborns at birth. Research on this process has increased exponentially in the last decade since its discovery almost a half a century ago. It has been found that autophagy is an important process in many diseases, continues to be at the forefront of research, and is clearly not fully understood. Our preliminary cell culture data in endothelial and epithelial cells show that a blockade of the de novo ceramide synthesis pathway, during treatment with an autophagy stimulus (cigarette smoke extract exposure), does not result in any reduction in autophagy or autophagic flux. Conversely, when acid sphingomyelinase (ASM) is pharmacologically inhibited, which prevents the generation of ceramide from sphingomyelin in an acidic environment, a profound increase in autophagy is observed. In this work, we hypothesize that (ASM) is an endogenous inhibitor of autophagy. ASM has two forms, a secreted form and a lysosomal form. N-terminal processing in the Golgi determines its cellular fate. In the lysosomal form, the phosphodiesterase is bound in the lysosomal membrane. The pharmacological inhibition mechanism is to release ASM from the membrane and allow other hydrolases to actively degrade the enzyme which, in turn, decreases the activity of ASM. This suggests

that either the activity of ASM is a regulator of autophagy or that the presence of ASM, activity aside, is required for the lysosomal nutrient sensing machinery (LYNUS) to function properly. Here, we show that ASM is, in fact, an endogenous inhibitor of autophagy in vitro. The phosphorylation status of P70 S6k, a downstream effector of mammalian target of rapamycin (mTOR), which is part of the LYNUS, shows that dissociation of ASM from the membrane regulates mTOR and disturbs the LYNUS in such a manner as to signal autophagy.

Irina Petrache, M.D., Chair

Table of Contents

List of Abbreviations

ASM	acid sphingomyelinase
mTOR	mammalian target of rapamycin
PI3k	phosphor inositol-3-kinase
BEAS2b	human immortalized bronchial epithelial cells
DMEM	Dulbecco's modified eagle media
FBS	fetal bovine serum
HPAEC	human pulmonary artery endothelial cells
PBS	phosphate buffered solution
CCK-8	cell counting kit-8
PI	propidium iodide
LC3B	microtubule associated protein light chain three beta

Introduction

Autophagy is a fundamental cellular process in which intracellular contents can be sequestered, degraded, and re-utilized to meet energy demands during periods of nutrient deprivation [1]. This process can be responsible for the degradation of long-lived proteins, lipids, protein aggregates, organelles, and even pathogens [2]. When this process is signaled, a double-bound membrane, a phagophore, starts forming around the contents to be degraded and, eventually, totally enclosing the contents and becoming a mature autophagosome [3]. This autophagosome will then fuse with a lysosome creating an autophagolysosome which will, in turn, degrade the cargo that has been supplied. The total process of autophagy, from formation of phagophore to degradation of autophagolysosome, has many steps with many autophagy related proteins (ATG) associated with each step. Proper evaluation of autophagic induction versus autophagic flux is imperative when evaluating this process [4].

Homeostatic autophagy is important for tissue function especially during stress, starvation, or infections [5]. Impaired or persistent autophagy may be pathogenic, leading to cell death and may play a role in various diseases such as cancer, metabolic, pulmonary, cardiovascular, and neurodegenerative diseases [5]. Emphysema, a pulmonary disease, is primarily caused by chronic cigarette smoking and is characterized by excessive apoptosis of structural cells of the lung such as endothelial cells and epithelial cells [6]. Recently, autophagy with decreased flux induced by cigarette smoke has been shown to be pathogenic in emphysema and to precede apoptosis [7]. Lungs with emphysema have increased levels of ceramide, a bioactive sphingolipid that has

been implicated in apoptosis [6]. There are reports in the literature that ceramide may also trigger autophagy [8]. To determine the importance of ceramide production in human lung structural cell autophagy, we focused on the enzyme acid sphingomyelinase (ASM), which produces ceramide from sphingomyelin. Two forms of ASM exist, a secreted and a lysosomal form that arise from the same protein precursor with destination determined by mannose-6-phosphate tagging and serine 508 phosphorylation [9]. In this work, we will focus only on the lysosomal form. The inhibition of ASM did not inhibit CS induced autophagy but rather markedly increased the formation of autophagolysosomes. That led us to the hypothesis that ASM, an enzyme that is responsible for producing pro-apoptotic ceramides, is an endogenous inhibitor of autophagy.

To investigate our hypothesis, we used imipramine a pharmacological inhibitor of ASM with an indirect mechanism of action [10]. Rather than a direct enzymatic inhibitor, imipramine through diffusion and hydrophobicity, aggregates in lysosomes and, through its organic weak base properties, dissociates ASM from the inner lysosomal membrane and allows quick proteolytic degradation of the enzyme leading to diminished activity [11].

To understand the mechanisms by which ASM may regulate autophagy, we focused on a major signaling pathway involved in autophagy, linking growth factor signaling to the machinery responsible for cell metabolism and proliferation [12]. This pathway is centered around the mammalian target of rapamycin (mTOR), a serine/threonine kinase that regulates cell growth, proliferation, and protein synthesis,

itself regulated by phosphor inositol-3-kinase (PI3k) and Akt activation [12]. Activation of Akt itself also serves to inhibit apoptosis by binding to BAX [13]. The resident location of mTOR in the cell is in the lysosomal nutrient sensing complex which is docked at the membrane of the lysosome [14]. If either availability of amino acids is limited or mTOR is not docked at the membrane, mTOR will not phosphorylate its downstream targets, halt translation and cell cycle, and will induce autophagy [15].

In this study, we show that ASM inhibition via imipramine leads to induction of autophagy in lung endothelial and epithelial cells, without decreasing the autophagic flux, moderately inhibiting proliferation and causing modest levels of apoptosis associated with inhibition of mTOR signaling (**Figure 1**). Elucidating the function of ASM as a stress-induced pro-apoptotic enzyme and concomitant endogenous inhibitor of autophagy may clarify the crosstalk between autophagy and apoptosis in health and disease.

Methods

Reagents

Unless otherwise stated, all reagents were purchased from Sigma-Aldrich (St. Louis, MO).

Cell Culture

Human immortalized bronchial epithelial cells (BEAS2b), were kindly provided by Dr. Augustine Choi (originally from ATCC), and cultured in Dulbecco's Modified Eagle Medium (DMEM) (Invitrogen, Carlsbad, CA) supplemented with 15% fetal bovine serum (FBS) (Thermo Fisher Scientific, Waltham, MA) and 1% penicillin/streptomycin. Primary human pulmonary artery endothelial cells (HPAEC) (Invitrogen) were cultured in Medium 200 (Invitrogen) containing Low Serum Growth Supplement (Invitrogen). Cells were kept in an incubator at 37°C and 100% humidity with 5% CO2.

For experiments, cells were grown in D100 dishes to 50-90% confluency. BEAS2b cells received media change of DMEM containing 2% FBS to simulate a low serum environment 2 hours prior to experimental procedures. HPAEC cells received fresh media at the time of experiment. Pre-treatments with the PI3k inhibitor, LY294002 (VWR, Radnor, PA) suspended in ethanol, and autophagsomal degradation inhibitor, chloroquine diphosphate (Thermo Fisher Scientific) suspended in water, were performed 1 hour prior to treatments with the ASM inhibitor imipramine (Calbiochem, San Diego, CA) suspended in water, and the autophagy inducer rapamycin, suspended in ethanol.

Immunoblotting

Cells were washed with ice-cold phosphate buffered saline (PBS) (Thermo Fisher Scientific) and gently scraped in ice-cold PBS and centrifuged at 20,000g for 10 minutes at 4°C. The PBS was then removed by aspiration, leaving a cell pellet that was snap-frozen in liquid nitrogen. Cell pellets were thawed on ice and lysed in a buffer containing 1% Triton-x (Thermo Fisher Scientific), 50mM TRIS (Invitrogen), and 150mM NaCl (Thermo Fisher Scientific). Cells were vortexed every 30 minutes for two hours on ice, centrifuged at high speed for 10 minutes at 4°C, supernatants removed, and the bicinchoninic acid assay (Peirce, Rockford, IL) was performed to determine total protein concentrations. Equal protein amounts between 5-20µg, were diluted with Laemmli 4X buffer (Boston Bioproducts, Ashland, MA) that contains sodium dodecyl sulfate and resolved by electrophoresis using Criterion 4-20% TGX pre-cast gels (Bio-Rad, Hercules, CA). Proteins were transferred to polyvinylidene fluoride membranes using a semi-dry transfer apparatus (Bio-Rad). Membranes were probed using the following primary antibodies (Cell Signaling, Beverly, MA, unless otherwise stated): phospho-P70 S6K (1:1,000), LC3B (1:20,000) (Sigma-Aldrich), P62-lck ligand (1:500) (BD Biosciences, San Jose, CA) and vinculin (1:20,000) (Calbiochem) or β-Actin (1:20,000) (Sigma-Aldrich) that was used as loading control. Appropriate secondary antibodies (ECL anti-rabbit or anti-mouse whole antibody horse radish peroxidase) (Thermo Fisher Scientific) (1:10,000) were used with ECL Prime/ECL Plus (Thermo Fisher Scientific) for chemiluminescent reactions. Images were taken using a ChemiDoc (Bio-Rad) XRS system with Image Lab software.

Electron Microscopy

Cells were washed with ice cold PBS solution and fixed in a 0.1M phosphate buffer solution containing two percent glutaraldehyde and two percent paraformaldehyde for 30 minutes at room temperature. Cells were then washed twice with PBS and gently scraped in PBS, centrifuged at high speed for 10 minutes and then transferred to the Electron Microscopy Core Facility at IU School of Medicine for embedding, cutting, and mounting on slides. Images were taken with a Tecnai G2 12 Bio Twin (FEI, Hillsboro, OR) equipped with an AMR CCD (Advanced Microscopy Techniques, Danvers, MA).

Cell Viability and Proliferation Assays

For the cell counting kit-8 (CCK-8) assay, cells were plated in a 96-well tissue culture plate at 5,000 cells per well and allowed to grow for 24 hours before treatment. Cells were then treated with CCK-8 reagent (Dojindo, Rockville, MD), a highly water-soluble tetrazolium salt, for 3 hours and then optical density at 450nm was determined by a micro-plate reader.

For the thymidine incorporation assay, cells were plated in a 96-well tissue culture plate and allowed to grow for 24 hours. Media (5 mL per treatment) was prepared and 125µL RPMI (Thermo Fisher Scientific) containing tritiated thymidine (Perkin Elmer, Waltham, MA; 1mL of tritiated thymidine in 24mL RPMI) was added. Media was then changed (200µL) in the 96-well plate and 25µL of tritiated thymidine (1µCi) in RPMI was added to each well. Following 24 hours of treatment, media was removed, and cells were washed with PBS, detached using TrypLE Select (Invitrogen),

and measured for radioactive thymidine incorporation via scintillation counting on a Wallac Microbeta (Boston, MA) 1450 Liquid Scintillation Counter. This experiment was performed in collaboration in Dr. Janice Blum's lab with special thanks to Lynette Guindon for performing the assay.

For the cell apoptosis assay (Annexin V staining), Cells were grown and treated in D100 dishes. Twenty minutes prior to assay, 400uL of 30% hydrogen peroxide was added to an untreated dish as positive control for apoptotic and necrotic gate parameters of the flow cytometer. Following harvesting, cells were stained for phosphatidylserine using Annexin V staining (Annexin V Kit 250 Samples; VWR), following manufacturer's protocol of washing cells in unicellular suspension with PBS containing calcium, magnesium, and 2% bovine serum albumin. Propidium iodide (PI) and fluorescently labeled Annexin V antibodies were then incubated for ten minutes in manufacturer's supplied binding buffer. Apoptosis was quantified by Annexin V/PI staining using a Cytomics FC500 cytofluorimeter (Beckman Coulter, Fullerton, CA) with CXP software. Special thanks to Daniela Petrusca for performing the assay.

Acid Sphingomyelinase Activity

Cells were grown and treated in D100 dishes with 50μM imipramine for four hours and the Amplex Red Sphingomyelinase Activity Kit (Invitrogen) was applied per manufacturer's protocol and fluorescence determined by a micro-plate reader.

Densitometry

All densitometry was performed using ImageJ software (Rasband, W.S., ImageJ, U. S. National Institutes of Health, Bethesda, MD, USA, http://imagej.nih.gov/ij/, 1997-2012).

Statistical Analysis

All statistical analyses of experiments with $n \geq 3$ were performed with The R Project for statistical computing (R Core Team (2013). R: A language and environment for statistical computing. R Foundation for Statistical Computing, Vienna, Austria. URL http://www.R-project.org/). When comparing 2 groups, a Welch Two Sample t test was used. When comparing multiple groups, a one-way ANOVA was performed with Tukey Honest Significant Difference post-hoc test with a p-value cutoff of 0.05 for significance.

Results

Disruption of ASM activation induces autophagy in a time- and dose-dependent manner in HPAEC

To investigate if autophagy is induced in a dose-dependent manner by pharmacological disruption and subsequent inhibition of ASM function with imipramine (**Figure 2**), we performed cell culture experiments using increasing doses of imipramine for 4 hours and probed total cell lysates for protein markers of autophagy via western blotting (**Figure 3A**). The onset of autophagy is typically marked by increased conversion of LC3B-I to LC3B-II via lipidation. We noted higher levels of LC3B-II following treatment with 50 or 100μM imipramine. Interestingly, concentrations of 200μM imipramine caused visible cell death and were not further analyzed. The western blot results were then quantified by densitometry (**Figure 3B**), which showed a statistical significance ($p \leq 0.01$) between 50μM and vehicle or 5μM imipramine concentrations. Similarly, imipramine concentrations of 100μM dose showed a statistically significant increase ($p \leq 0.001$) of LC3B-II compared to vehicle, 50μM dose, or 5μM. To investigate the kinetics of imipramine-induced autophagy, we performed cell culture experiments with 50μM imipramine at various time points (**Figure 3C**). These results have been quantified by densitometry, which demonstrated statistical significance ($p \leq 0.01$) between imipramine treatment and vehicle at both 4 hour and 24 hour time-points (Figure 3D).

ASM inhibition-induced autophagy is not cell-type specific

To determine if ASM inhibition induces autophagy in other human cell types, we investigated lung bronchial epithelial cells using the BEAS2b cell line. Imipramine

treatment induced similar marked increases in LC3B-II versus vehicle in epithelial cells (**Figure 4A**) as we noted in endothelial cells. Quantification by densitometry showed statistically significant increase in LC3B-II accumulation ($p \leq 0.05$) (**Figure 4B**). To further confirm the presence of autophagy induced by imipramine, we performed electron microscopy to visualize intracellular morphological changes pathognomonic for autophagy (**Figure 4C**). In the vehicle-treated control conditions, we noted normal cellular morphology, with healthy appearing endoplasmic reticulum (e), nuclei (n), and mitochondria (m). In the imipramine treated-cells, we noted numerous multi-vesicular bodies indicative of autophagy. Interestingly, we noted that the euchromatin and heterochromatin in nuclei of imipramine-treated cells had a different distribution than that of normal nuclei, suggesting potential epigenetic changes in addition to autophagy.

Impact of ASM inhibition on autophagic flux

To investigate the effects of ASM inhibition on autophagic flux, we treated HPAEC with imipramine (50μM; 4 hours), using the following control conditions: untreated cells, vehicle treatment, and chloroquine (an autophagolysosome degradation or flux inhibitor). In addition, we used the PI3K inhibitor LY294002 (100μM) as a typical inhibitor of autophagy upstream of mTOR. If imipramine inhibits autophagic flux, we would expect treatment with choloroquine to not exacerbate the accumulation of LC3B-II or p62. On the contrary, if imipramine does not inhibit the flux, administration of chloroquine, which blocks the flux, will further increase LC3B-II levels when co-administered with imipramine at the four hour time point. As expected, imipramine treatment increased LC3B-II, without a marked effect on p62 accumulation (**Figure 5A**).

The addition of chloroquine to imipramine, although not significantly affecting p62 levels (**Figure 5B**), markedly increased LC3B-II accumulation when compared to imipramine alone, and effect which was statistically significant when quantified by densitometry (**Figure 5C**). This suggested that cells treated with imipramine do not exhibit an impaired autophagic flux. Interestingly, LY294002 did not inhibit autophagy induced by imipramine, suggesting imipramine may act downstream of PI3K to induce autophagy.

ASM inhibition-induced autophagy is associated with mTOR signaling

To investigate if the mTOR pathway is affected by ASM inhibition, we used as a positive control rapamycin, a typical mTOR inhibitor, which reduces the phosphorylation of P70 S6 kinase (p-S6k) that is needed for cap-dependent translation and cell cycle progression. We first performed a dose curve of rapamycin (50-500 nM) and determined its effect on S6k phosphorylation and autophagy (LC3BI lipidation) (**Figure 6A**). Rapamycin at concentrations of 100nM or 500nM increased levels of LC3B-II and decreased levels of LC3B-I, indicating autophagy. The PI3k inhibitor LY294002 administered in concentrations of 100μM, but not of 50μM appeared to slightly reduce the conversion of LC3B-I to LC3B-II induced by rapamycin (100 nM; less so at 500 nM), without affecting the marked inhibitory effect of rapamycin on p-S6k. Interestingly, treatment with the ASM inhibitor imipramine, dose-dependently (**Figure 6B**) decreased p-S6k levels as early as 1 hour with a sustained effect for up to 24 hours (**Figure 6C**), indicating an important effect of ASM on mTOR activation.

Effect of ASM inactivation on fundamental cell functions, such as cell proliferation, viability, and apoptosis

We next determined if autophagy induced by ASM inhibition is associated with alterations in cell proliferation rates and overall cell fate. Since autophagy is typically associated with inhibition of cell proliferation (via mTOR pathway) we first measured thymidine incorporation in cells treated with imipramine and noted a mild reduction in cell proliferation at 24 hours, which was further impaired by adding a blocker of autophagy flux with chloroquine (**Figure 7A**). As expected, another autophagy inducer, the mTOR inhibitor rapamycin also reduced cell proliferation, whereas the PI3K inhibitor LY294002 uniformly and markedly lowered proliferation alone or when combined with other treatments. To understand if the imipramine-associated autophagy and decreased proliferation led to decreased cell viability, we used a CCK-8 assay, which is a measure of total intracellular dehydrogenase activity and is thus an indirect measure of viability. Imipramine-treated cells exhibited mild decreases in cellular viability at 24 hours, to a similar degree as those treated with chloroquine, whereas rapamycin-treated cells show a modest increase (**Figure 7B**). Finally, to determine if the mild decrease in cell proliferation and viability induced by the pro-autophagic imipramine is paralleled by an increase in apoptosis, we quantified externalization of phosphatidylserine at the plasma membrane using Annexin V staining. Imipramine-treated cells exhibited an increasing trend in apoptosis at 24 hours (**Figure 7C**). This effect was augmented by the addition of the PI3K inhibitor LY294002.

Figure 1

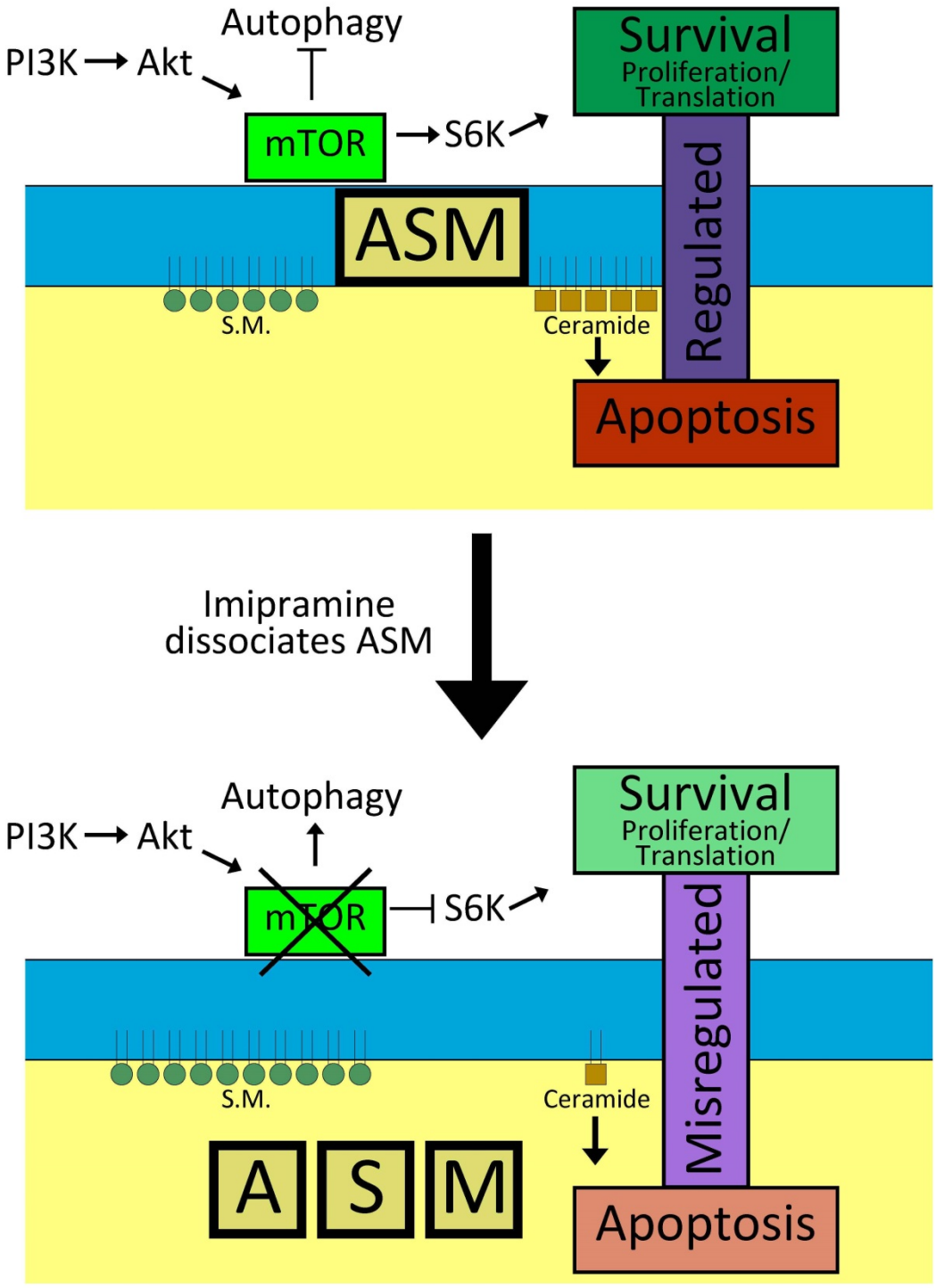
Autophagy
PI3K
Akt
mTOR
S6K
Survival
Proliferation/
Translation
Regulated
ASM
S.M.
Ceramide
Apoptosis
Imipramine
dissociates ASM
Autophagy
PI3K
Akt
mTOR
S6K
Survival
Proliferation/
Translation
Misregulated
S.M.
Ceramide
A
S
M
Apoptosis

Figure 1 Mechanism of loss of mTOR signaling due to ASM inhibition

The mechanism of ASM inhibition involves its dissociation from the membrane and subsequent mTOR loss-of-function. The homeostatic relationship between survival and apoptosis is disrupted by a decrease in the cell's ability to readily produce pro-apoptotic ceramides from existing sphingomyelin pools with a concomitant loss of S6k phosphorylation producing misregulated cell survival/death signaling.

Figure 2

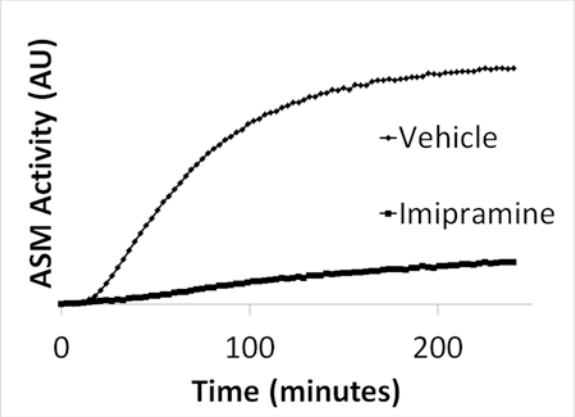

Figure 2 Treatment with imipramine reduces ASM activity

HPAEC were treated for 4 hours with imipramine and ASM activity measured. Data represents single experiment. Imipramine diminishes ASM activity.

Figure 3A

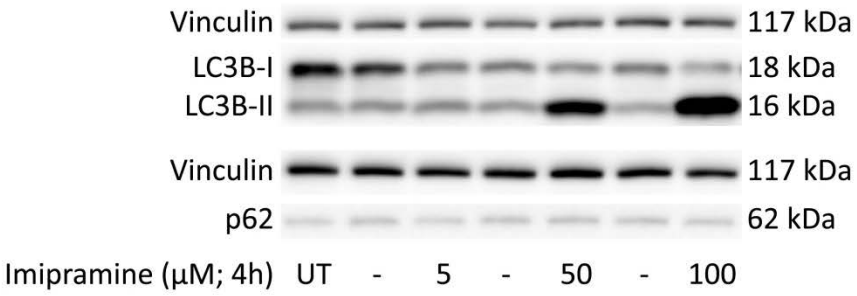

Figure 3B

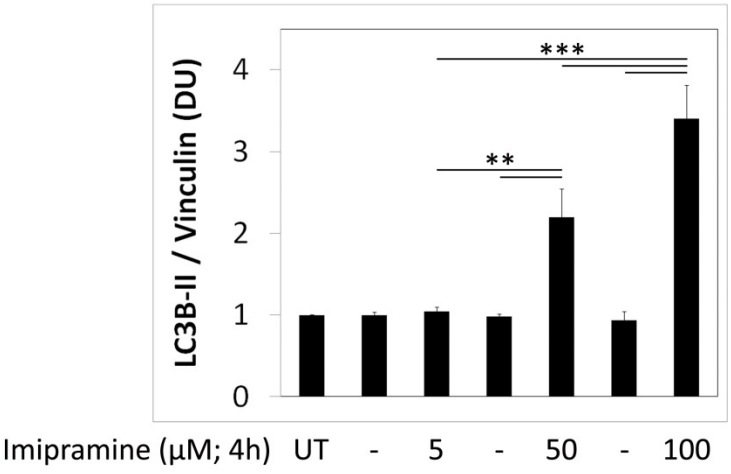

Figure 3A Autophagy is induced in a dose-dependent manner

HPAEC were treated for four hours with indicated doses of imipramine. Whole cell lysates were used to probe for changes in LC3B-II and p62 via western blotting. Vinculin was used as a loading control. LC3B-II levels increase with 50 and 100µM treatment of imipramine. This is a representative image of three experiments.

Figure 3B Quantification of western blot results

Image J was used to perform densitometry on protein bands in **Figure 1A**. LC3B-II had significant increase in the 50 and 100µM dosage. All LC3B-II levels were normalized by their respective vinculin loading controls. Data are represented as the average of three experiments, error bars represent standard error of the mean, n=3, ** = $p \leq 0.01$, *** = $p \leq 0.001$.

Figure 3C

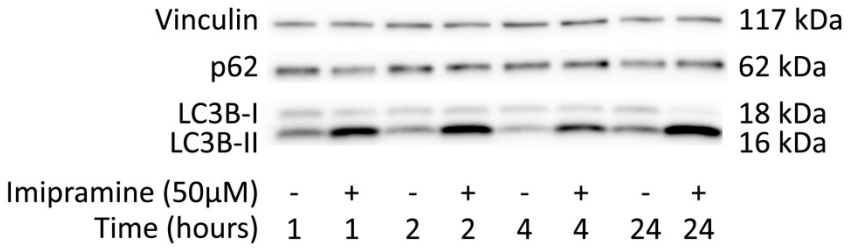

Figure 3D

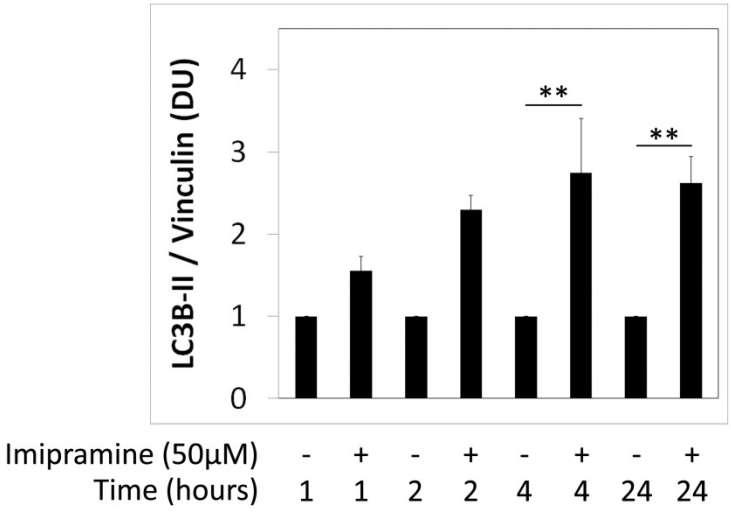

Figure 3C Kinetics of imipramine induced autophagy

HPAEC were treated with 50μM imipramine for indicated periods of time. Whole cell lysates were used to probe for changes in LC3B-II and p62. Vinculin was used as a loading control. This is a representative image of three experiments. LC3B-II levels increase with imipramine treatment.

Figure 3D Quantification of LC3B-II by densitometry

Image J was used to perform densitometry on protein bands in **Figure 1C**. LC3B-II had significant increase over that of control at the four and 24 hour time points. Although the average values of LC3B-II levels are higher at one and two hours are larger than their respective vehicle controls, the values are not significantly different. All LC3B-II levels were normalized by their respective β-Actin loading control. Data are represented as the average of three experiments, error bars represent standard error of the mean, n=3, ** = $p \leq 0.01$.

Figure 4A

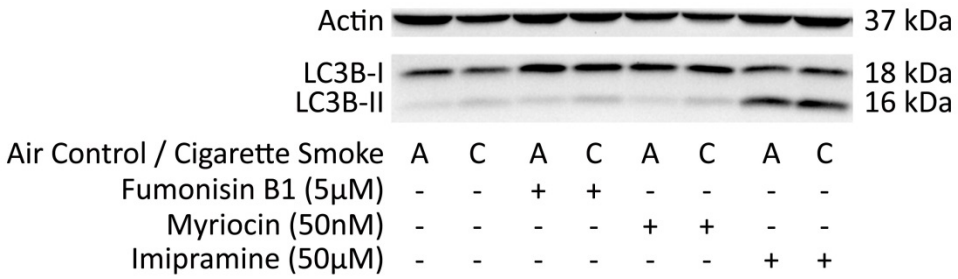

Figure 4B

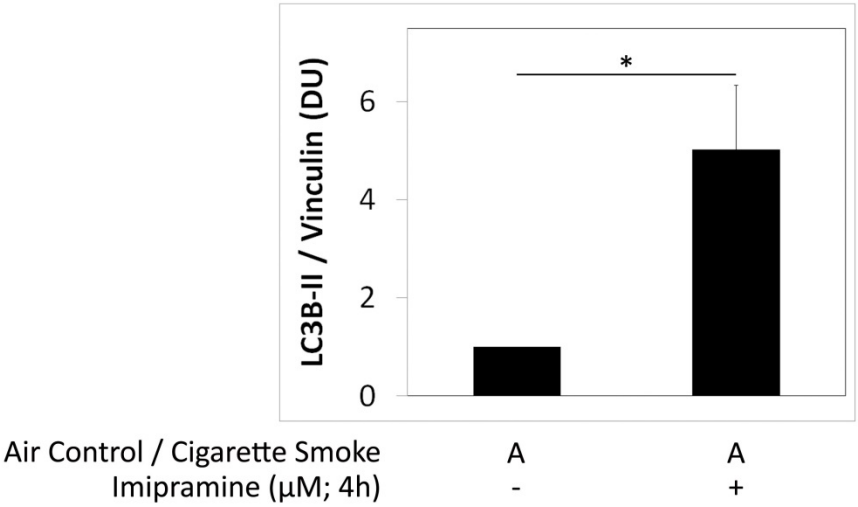

Figure 4A Imipramine induces autophagy in BEAS2b cells

BEAS2b were treated with 50μM imipramine, 5μM FB1, or 50nM Myriocin for four hours in the presence of air control extract (A) or cigarette smoke extract (C). Whole cell lysates were used to probe for changes in LC3B-II and p62. β-Actin was used as a loading control. This is a representative image of six experiments. LC3B-II is increased in both air control and cigarette smoke treated cells that were exposed to imipramine.

Figure 4B Quantification of LC3B-II by densitometry

Image J was used to perform densitometry on protein bands in **Figure 4A**. LC3B-II had significant increase over that of control. All LC3B-II levels were normalized by their respective β-Actin loading controls. Data represent averages of 6 experiments and error bars represent standard error of the mean, n=6, * = $p \leq 0.05$.

Figure 4C

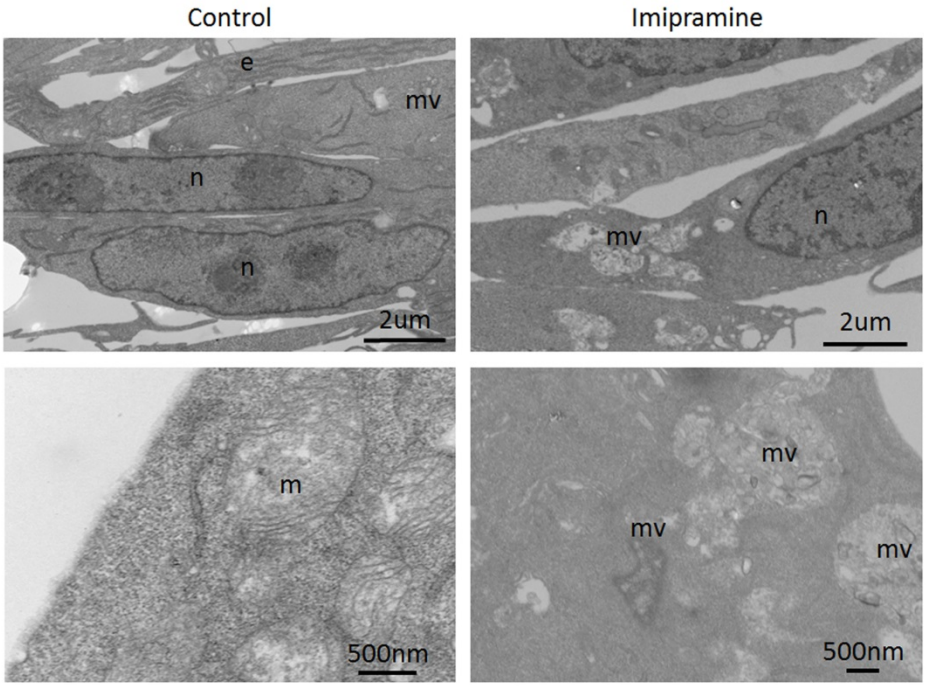

Figure 4C Electron microscopy of imipramine induced autophagy

BEAS2b cells were fixed and viewed by electron microscopy. Organelles are marked by lower case letters e (endoplasmic reticulum), n (nucleus), m (mitochondria). Autophagosomes (a), lysosomes (l), and autophagolysosomes (al) are also marked. The left two panels are control and the right two treated with 50µM imipramine. The scale bar represents 2µm in the top panels and 500nm in the bottom panels. The control panels show normal, healthy cells. The imipramine treated cells show an over-abundance of multi-vesicular structures as well as changes in the distribution of euchromatin (light areas inside nucleus) and heterochromatin (dark areas inside nucleus) patterns indicating different epigenetic processes. Images are representative of 10 images taken per treatment.

Figure 5A

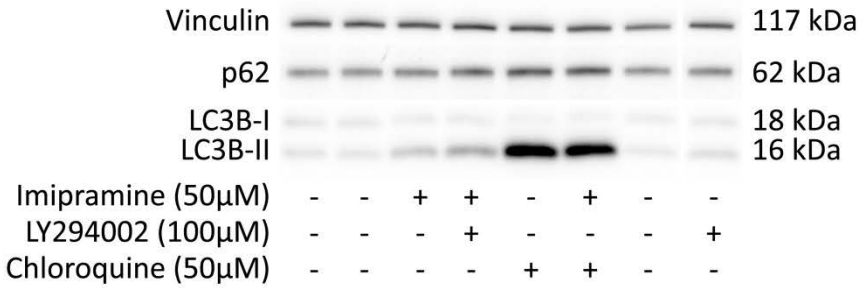

Figure 5B

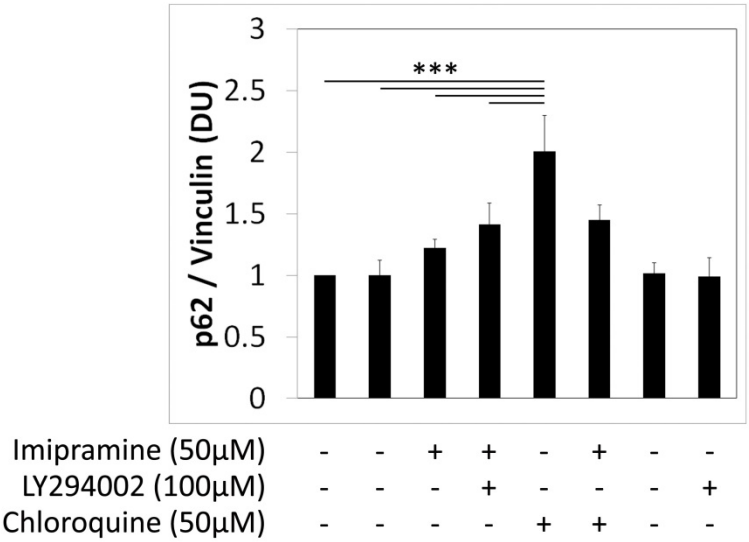

Figure 5C

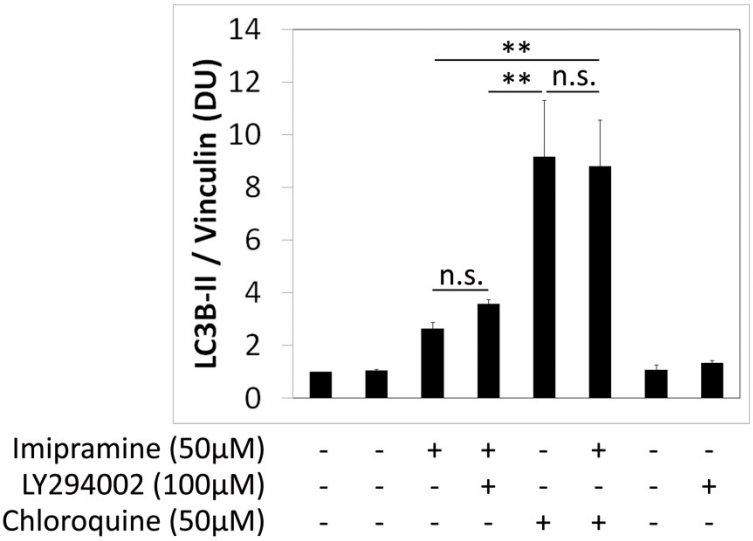

Figure 5A Impact of ASM inhibition on autophagic flux

HPAEC were treated with 50μM imipramine for four hours with and without pre-treatment with LY294002 or chloroquine. Whole cell lysates were used to probe for changes in LC3B-II and p62. Vinculin was used as a loading control. Image is representative of three experiments. LC3B-II is markedly increased with chloroquine treatment with or without the addition of imipramine over that of imipramine treatment alone.

Figure 5B Quantification of LC3B-II by densitometry

Image J was used to perform densitometry on protein bands in **Figure 5A**. All LC3B-II levels were normalized by their respective vinculin loading controls. Addition of chloroquine to imipramine treatment resulted in a significant 3-fold increase in LC3B-II over imipramine treated cells and a significant 6-fold increase over vehicle. There was no significant difference between chloroquine and chloroquine with imipramine treatment or between imipramine and imipramine with LY294002 treatment. Data represent averages of 3 experiments and error bars represent standard error of the mean, n=3, n.s. = no significance, ** = $p \leq 0.01$.

Figure 5C Quantification of p62 by densitometry

Image J was used to perform densitometry on protein bands in **Figure 5A**. In the four hour experiment, p62 had significant increase only in the cells treated with both imipramine and chloroquine. All p62 levels were normalized by their respective vinculin loading controls. Data represent averages of 3 experiments and error bars represent standard error of the mean, n.s. = no significance, *** = $p \leq 0.001$.

Figure 6A

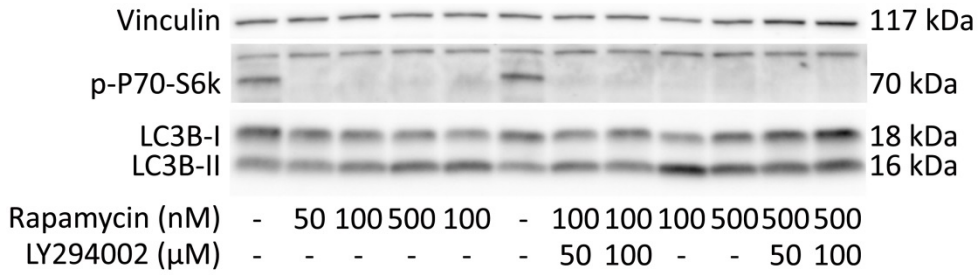

Figure 6B

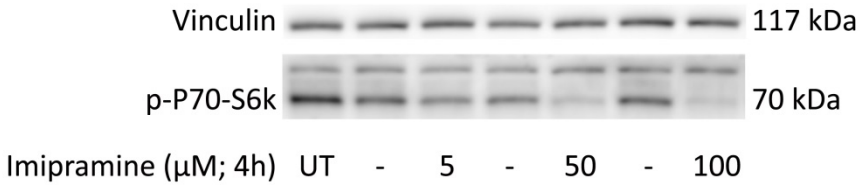

Figure 6C

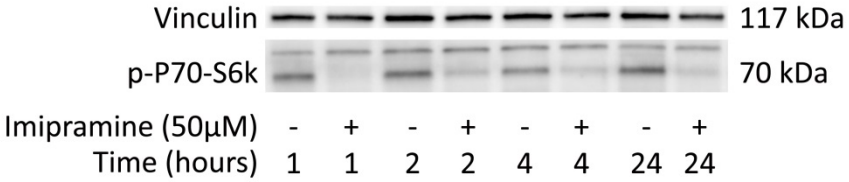

Figure 6A Rapamycin and LY294002 effects on LC3B-II lipidation and P70 S6k phosphorylation

HPAEC were treated with varying concentrations of rapamycin and two concentration of rapamycin were chosen to also treat with two concentrations of LY294002. Whole cell lysates were used to probe for changes in LC3B-II and phosphorylated P70 S6k. Vinculin was used as a loading control. This image represents one experiment. Levels of LC3B-II were increased with the 100 and 500nM treatment of rapamycin. Addition of 100μM LY294002 reduced LC3B-II levels induced by the 100nM rapamycin treatment.

Figure 6B Dose dependent decrease in phosphorylated P70 S6k by imipramine

HPAEC were treated for four hours with indicated doses of imipramine. Whole cell lysates were used to probe for changes in phosphorylated P70 S6k. Vinculin was used as a loading control. Data is representative of one experiment. Phosphorylation of P70 S6k was reduced with 50 and 100μM treatments.

Figure 6C Time dependent decrease in phosphorylated P70 S6k by imipramine

HPAEC were treated with 50μM imipramine for indicated periods of time. Whole cell lysates were used to probe for changes in phosphorylated P70 S6k. Vinculin was used as a loading control. Data is representative of one experiment. All 50μM imipramine treatments reduced the levels of phosphorylated P70 S6k.

Figure 7A

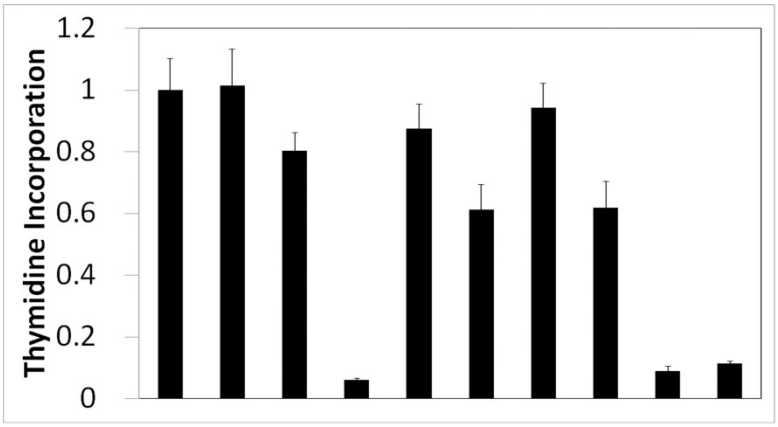

Imipramine (50µM)	-	-	+	+	-	+	-	-	-	-
LY294002 (100µM)	-	-	-	+	-	-	-	-	+	+
Chloroquine (50µM)	-	-	-	-	+	+	-	-	-	-
Rapamycin (100nM)	-	-	-	-	-	-	-	+	-	+

Figure 7A ASM inhibition decreases proliferation

HPAEC cells were incubated with tritiated thymidine under 24 hour experimental conditions and radioactive thymidine incorporation was quantified by scintillation counting. Data represents a single experiment performed in octuplicate. Imipramine and rapamycin treatments lowered proliferation while all treatments with LY294002 greatly reduced proliferation.

Figure 7B

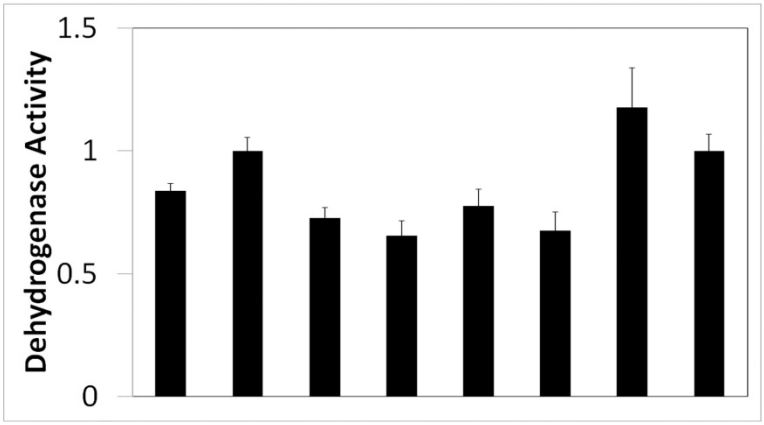

Imipramine (50µM)	-	-	+	+	-	+	-	-
3MA (5mM)	-	-	-	+	-	-	-	-
Chloroquine (50µM)	-	-	-	-	+	+	-	-
Rapamycin (100nM)	-	-	-	-	-	-	+	-

Figure 7B ASM inhibition causes mild decrease in cell viability

HPAEC were incubated with indicated treatments for 24 hours and cell viability was indirectly measure by total dehydrogenase activity. Data represent a single experiment performed in octuplicate. Imipramine shows a slight decrease in number of viable cells.

Figure 7C

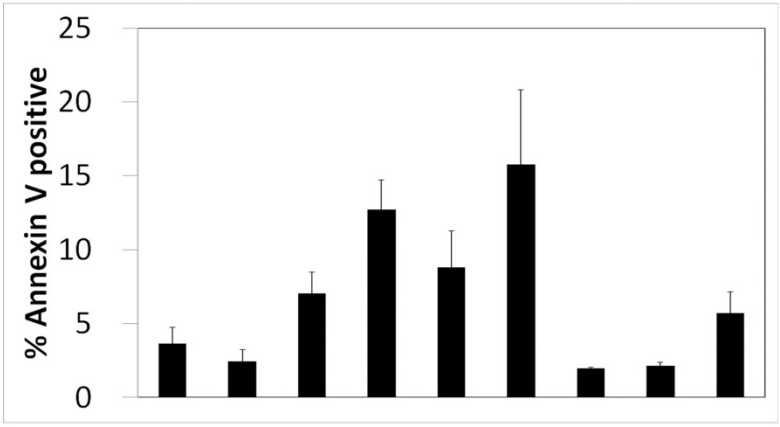
% Annexin V positive
25
20
15
10
5
0
Imipramine (50µM) - - + + - + - - -
LY294002 (100µM) - - - + - - - - +
Chloroquine (50µM) - - - - + + - - -
Rapamycin (100nM) - - - - - - - + -

Figure 7C ASM inhibition exhibits slight increase in apoptosis

HPAEC were incubated with indicated treatments for 24 hours and total apoptotic events were measured by Annexin V staining. Data represent three experiments. Imipramine shows a slight, non-significant increase in number of apoptotic cells.

Discussion

Here we have shown that disruption of ASM from the lysosomal membrane induces autophagy associated with inhibition of mTOR signaling. This autophagic response is followed by decreased cell proliferation with a modest loss of cell viability and increased apoptosis. These results implicate ASM as an endogenous inhibitor of autophagy.

Our work was conducted in primary human lung endothelial and epithelial cells given our interest in the pathogenesis of lung diseases such as emphysema, a manifestation of chronic obstructive pulmonary disease characterized by airspace destruction through excessive apoptosis of these two types of structural cells. The implications of our findings to emphysema are yet to be determined. Typically, cigarette smoking induces both autophagy with an improper flux and apoptosis and activates ASM. Treatment with ASM inhibitors may alleviate apoptosis, but are unlikely to inhibit autophagy, rather they activate it. In addition, there are many individuals who are taking imipramine as an antidepressant. While adverse effects of this drug on lung function have not been reported, it would be interesting to investigate its effect on other conditions in which autophagy is important, such as lung or other cancers, neurodegenerative diseases, or adaptations to physical exercise.

Commonly, the research surrounding ASM is centered on the production of ceramide via activation of this enzyme. There is little known about the requirement for the homeostatic role of lysosomal ASM in cell fate or autophagy. We used the ASM inhibitor imipramine because it dissociates ASM from the membrane and diminishes its

activity without affecting other lysosomal hydrolases [16]. Using this inhibitor, our results suggest that fundamental mTOR dependent cell functions such as cell proliferation and translation are regulated by ASM presence in the lysosomal membrane. This conclusion will have to be confirmed in future studies using cell fractionation and immunofluorescence for ASM presence in the lysosomes as well as by molecular tools of lysosomal ASM loss and re-gain of function.

Our results are supported by a prior publication by Jeon et al. which showed that imipramine (used in similar concentrations as in our experiments) induced autophagic cell death in human glioma cells via mTOR inhibition [17]. In the context of this research, Wuwonqse et al. coupled synaptic degeneration with depression and autophagy-based removal of damaged synaptic proteins suggesting a therapeutic role for antidepressants [18]. In a study by Rossi et al., desmethylclomipramine, a similar drug to imipramine, induces accumulation of autophagic markers by blocking autophagic flux in HeLa cells [19]. Our study is performed in a primary, non-immortalized, non-cancerous lung cell line and co-treatment with imipramine and chloroquine shows a marked increase in abundance of LC3B-II over treatment with imipramine alone which suggests that autophagic flux is not impaired when autophagy is induced by ASM inhibition.

Imipramine and rapamycin appear to have similar effect on the signaling produced by the mTOR pathway by looking at LC3B-II and the downstream effector p-S6k. While rapamycin directly inhibits mTOR from functioning, imipramine dissociates ASM from the lysosomal membrane indicating a mechanical relation between ASM and the mTOR complex. The addition of chloroquine, a typical autophagic flux inhibitor, to

imipramine treatment markedly increased the presence of autophagosomes, indicating that ASM disruption induces autophagy without impairing the autophagic flux.

This report is limited by possible non-specific effects of a pharmacological inhibitor such as imipramine. A proper complement to this study would be that of small interfering RNA to prove specificity. Also, cell culture experiments are a great prelude to animal experiments, but are simple when compared to the complexity of an animal model. These limitations will be addressed in future, already planned experiments.

In conclusion, there is an intimate link between ASM and mTOR signaling which may regulate the onset and fate of autophagy. The ASM inhibitor imipramine is a potent inducer of autophagy that does not block autophagic flux and this effect may allow its application in conditions in which such an effect is desirable, such as conditions of improper protein folding.

References

[1] N. Mizushima, "Autophagy: process and function," Genes & Development, vol. 21, no. 22, pp. 2861-2873, 2007.

[2] A. Patel, D. Morse and A. Choi., "Regulation and Functional Significance of Autophagy in Respiratory Cell Biology and Disease," American Journal of Respiratory Cell Molecular Biology, vol. 48, no. 1, pp. 1-9, 2013.

[3] S. A. Tooze and T. Yoshimori, "The Origin of the Autophagosomal Membrane, "Nature Cell Biology, vol. 12, no. 9, pp. 831-835, 2010.

[4] D. J. Klionsky, H. Abeliovich, P. Agostinis, D. K. Agrawal, G. Aliev, D. S. Askew, M. Baba, E. H. Baehrecke, B. A. Bahr, A. Ballabio, B. A. Bamber, D. C. Bassham, E. Bergamini, X. Bi, M. Biard-Piechaczyk, J. S. Blum, D. E. Bredesen, J. L. Brodsky, J. H. Brumell, U. T. Brunk, W. Bursch, N. Camougrand, E. Cebollero, F. Cecconi, Y. Chen, L. Chin, A. Choi, C. T. Chu, J. Chung, P. G.H. Clarke, R. S.B. Clark, S. G. Clarke, C. Clavé, J. L. Cleveland, P. Codogno, M. I. Colombo, A. Coto-Montes, J. M. Cregg, A. Maria Cuervo, J. Debnath, F. Demarchi, P. B. Dennis, P. A. Dennis, V. Deretic, R. J. Devenish, F. Di Sano, J. F. Dice, M. DiFiglia, S. Dinesh-Kumar, C. W. Distelhorst, M. Djavaheri-Mergny, F. C. Dorsey, W. Dröge, M. Dron, W. A. Dunn, Jr, M. Duszenko, N. T. Eissa, Z.Elazar, A. Esclatine, E. L. Eskelinen, L. Fésüs, K. D. Finley, J. M. Fuentes, J.Fueyo, K.Fujisaki, B. Galliot, F.B. Gao, D.A. Gewirtz, S. B. Gibson, A. Gohla, A. L. Goldberg, R. Gonzalez, C. González-Estévez, S. Gorski, R. A. Gottlieb, D. Häussinger, Y. W. He, K. Heidenreich, J. A. Hill, M. Høyer-Hansen, X. Hu, W. P. Huang, A. Iwasaki, M. Jäättelä, W. T. Jackson, X. Jiang, S. Jin, T. Johansen, J. U. Jung, M. Kadowaki, C. Kang, A. Kelekar, D. H. Kessel, J. A.K.W. Kiel, H. P.

Kim, A. Kimchi, T. J. Kinsella, K. Kiselyov, K. Kitamoto, E. Knecht, M. Komatsu, E. Kominami, S. Kondo, A. L. Kovács, G. Kroemer, C. Y. Kuan, R. Kumar, M. Kundu, J. Landry, M. Laporte, W. Le, H. Y. Lei, M. J. Lenardo, B. Levine, A. Lieberman, K. L. Lim, F. C. Lin, W. Liou, L. F. Liu, G. Lopez-Berestein, C. López-Otín, B. Lu, K. F. Macleod, W. Malorni, W. Martinet, K. Matsuoka, J. Mautner, A. J. Meijer, A. Meléndez, P. Michels, G. Miotto, W. P. Mistiaen, N. Mizushima, B. Mograbi, I. Monastyrska, M. N. Moore, P. I. Moreira, Y. Moriyasu, T. Motyl, C. Münz, L. O. Murphy, N. I. Naqvi, T. P. Neufeld, I. Nishino, R. A. Nixon, T. Noda, B. Nürnberg, M. Ogawa, N. L. Oleinick, L. J. Olsen, B. Ozpolat, S. Paglin, G. E. Palmer, I. Papassideri, M. Parkes, D. H. Perlmutter, G. Perry, M. Piacentini, R. Pinkas-Kramarski, M. Prescott, T. Proikas-Cezanne, N. Raben, A. Rami, F. Reggiori, B. Rohrer, D. C. Rubinsztein, K. M. Ryan, J. Sadoshima, H. Sakagami, Y. Sakai, M. Sandri, C. Sasakawa, M. Sass, C. Schneider, P. O. S., O. Seleverstov, J. Settleman, J. J. Shacka, I. M. Shapiro, A. Sibirny, E. C. M. Silva-Zacarin, H. U. Simon, C. Simone, A. Simonsen, M. A. Smith, K. Spanel-Borowski, V. Srinivas, M. Steeves, H. Stenmark, P. E. Stromhaug, C. S. Subauste, S. Sugimoto, D. Sulzer, T. Suzuki, M. S. Swanson, I. Tabas, F. Takeshita, N. J. Talbot, Z. Tallóczy, K. Tanaka, K. Tanaka, I. Tanida, G. S. Taylor, J. P. Taylor, A. Terman, G. Tettamanti, C. B. Thompson, M. Thumm, A. M. Tolkovsky, S. A. Tooze, R. Truant, L. V. Tumanovska, Y. Uchiyama, T. Ueno, N. L. Uzcátegui, I. van der Klei, E. C. Vaquero, T. Vellai, M. W. Vogel, H. G. Wang, P. Webster, J. W. Wiley, Z. Xi, G. Xiao, J. Yahalom, J. M. Yang, G. Yap, X. M. Yin, T. Yoshimori, L. Yu, Z. Yue, M. Yuzaki, O. Zabirnyk, X. Zheng, X. Zhu, R. L. Deter, "Guidelines for the Use and Interpretation of Assays for Monitoring Autophagy in Higher Eukaryotes," Autophagy, vol. 8, no. 4, pp. 151-175, 2008.

[5] A. Choi, S. W. Ryter and B. Levine, "Autophagy in Human Health and Disease, "New England Journal of Medicine, vol. 368, no. 7, pp. 651-662, 2013.

[6] I. Petrache, L. Z. T. M. A. R. C. C. V Natarajan and E. B. R. T. W.C. Hubbard, "Ceramide Upregulation Causes Pulmonary Cell Apoptosis and Emphysema-Like Disease in Mice," Nature Medicine, vol. 11, no. 5, pp. 491-498, 2005.

[7] M. M. Monick, L. S. Powers, K. Walters, N. Lovan, M. Zhang, A. Gerke, S. Hansdottir and G. W. Hunninghake, "Identification of an Autophagy Defect in Smokers' Alveolar Macrophages," Journal of Immunology, vol. 185, no. 9, pp. 5425-5435, 2010.

[8] S. Pattingre, C. Bauvy, T. Levade, B. Levine and P. Codogno, "Ceramide-Induced Autophagy: to Junk or to Protect Cells," Autophagy, vol. 5, no. 4, pp. 558-560, 2009.

[9] R. Jenkins, D. Canals, J. Idkowiak-Baldys, F. Simbari, P. Roddy, D. Perry, K. Kitatani, C. Luberto and Y. Hannun, "Regulated Secretion of Acid Sphingomyelinase: Implications for Selectivity of Ceramide Formation," Journal of Biological Chemistry, vol. 285, no. 46, pp. 35706-35718, 2010.

[10] R. Hurwitz, K. Ferlinz and K. Sandhoff, "The Tricyclic Antidepressant Desipramine Causes Proteolytic Degradation of Lysosomal Sphingomyelinase in Human Fibroblasts," Biological Chemistry Hoppe Seyler, vol. 375, no. 7, pp. 447-450, 1994.

[11] J. Kornhuber, P. Tripal, M. Reichel, L. Terfloth, S. Bleich, J. Wiltfang and E. Gulbins, "Identification of New Functional Inhibitors of Acid Sphingomyelinase Using a Structure-Property-Activity Relation Model," Journal of Medicine Chemistry, vol. 51, no. 2, pp. 219-237, 2008.

[12] G. G. Chiang and R. T. Abraham, "Phosphorylation of Mammalian Target of Rapamycin (mTOR) at Ser-2448 Is Mediated by p70S6 Kinase," Journal of Biological Chemistry, vol. 280, no. 27, pp. 25485-25490, 2005.

[13] S. Gardai, D. Hildeman, S. Frankel, B. Whitlock, S. Frasch, N. Borregaard, P. Marrack, D. Bratton and P. Henson, "Phosphorylation of Bax Ser184 by Akt Regulates its Activity and Apoptosis in Neutrophils," Journal of Biological Chemistry, vol. 279, no. 20, pp. 21085-21095, 2004.

[14] C. Settembre, A. Fraldi, D. Medina and A. Ballabio, "Signals from the Lysosome: a Contol Centre for Cellular Clearance and Energy Metabolism," Nature Review Molecular Cell Biology, vol. 14, no. 5, pp. 283-296, 2013.

[15] C. Canq, Y. Zhou, B. Navarro, Y. Seo, K. Aranda, L. Shi, S. Battaglia-Hsu, I. Nissim, D. Clapham and D. Ren, "mTOR Regulates Lysosomal ATP-Sensitive Two-Pore Na(+) Channels to Adapt to Metabolic State," Cell, vol. 152, no. 4, pp. 778-790, 2013.

[16] S. Albouz, J. Hauw, Y. Berwald-Netter, J. Boutry, R. Bourdon and N. Baumann, "Tricyclic Antidepressants Induce Sphingomyelinase Deficiency in Fibroblast and Neuroblastoma Cell Cultures," Biomedicine, vol. 35, no. 7-8, pp. 218-220, 1981.

[17] S. Jeon, S. Kim, Y. Kim, Y. Kim, Y. Lim, Y. Lee and S. Shin, "The Tricyclic Antidepressant Imipramine Induces Autophagic Cell Death in U-87MG Glioma Cells," Biochem Biophys Res Commun, vol. 413, no. 2, pp. 311-317, 2011.

[18] S. Wuwonqse, S. Cheng, G. Wong, C. Hung, N. Zhang, Y. Ho, A. Law and R. Chang, "Effects of Corticosterone and Amyloid-Beta on Proteins Essential for Synaptic Function: Implications for Depression and Alzheimer's Disease," Biochim Biophys Acta, vol. 1832, no. 12, pp. 2245-2256, 2013.

Curriculum Vitae

MATTHEW JOSE JUSTICE

EDUCATION

December 2013: **Master of Science – Biochemistry & Molecular Biology**

Indiana University, Indianapolis, Indiana

Project 1: Role of acid sphingomyelinase in autophagy (Thesis project).

Project 2: Role of sphingolipids in cigarette smoke-induced autophagy.

August 2009: **Master of Science – Physics**

Purdue University, Indianapolis, Indiana

Project 1: To study the phase separation in binary mixtures of bipolar and monopolar lipid dispersions;

Project 2: To examine the effect of ceramide on membrane cell fusion and the relevance to cellular apoptosis.

May 2006: **Bachelor of Science – Physics**

Indiana University, South Bend, IN

Senior Research Project: To design and implement a focal plane for a recoil mass separator in a collaborative arrangement with the University of Notre Dame.

RESEARCH WORK EXPERIENCE

2009 – 2012: **Research Technician**, Indiana University School of Medicine, Indianapolis.

- Worked on a project investigating sphingolipids in the lung in murine and cell culture models (human bronchial epithelial cells and human pulmonary artery cells) of cigarette smoke-induced injury, using the following techniques: Cell Culture, Immunoblotting, Immuno-fluorescence, Electron Microscopy, Experimental Design and Planning, Rodent Experiments and Harvesting.
- Discussed the novelty and quality of published research manuscripts via presentations at Journal Club.

2007 – 2009: **Research Assistant**, Purdue University, Indianapolis

- Measured molecular interactions in several systems: biological membranes, proteins, and fuel cell nanoparticles.
- Experimental methods included small angle x-ray scattering using a Bruker Nanostar x-ray system, NMR spectroscopy using a Varian 300 MHz spectrometer, and calorimetry using a Microcal isothermal titration calorimeter. Designed, implemented, and optimized a temperature control system for the Bruker Nanostar instrument.

2005 – 2006: **Student Researcher,** University of Notre Dame

- Designed, optimized, and begun implementation of the focal plane for a recoil mass separator.

OTHER WORK EXPERIENCE

2013 – Present: **Adjunct Professor**, Butler University, Indianapolis, Indiana

Undergraduate Courses taught:

- NW -262-PH – The Physical World – Lecture and Lab (5 hours); general Physics course for non-Physics majors.

2006-2007: Quality Control Supervisor, Patrick Industries, Mishawaka, Indiana.

2004-2006: Manufacturing, Forge Industrial Staffing, South Bend, Indiana.

MANUSCRIPTS

Brownholland DP, Longo GS, Struts AV, **Justice MJ**, Szleifer I, Petrache HI, Brown MF, Thompson DH. Phase Separation in Binary Mixtures of Bipolar and Monopolar Lipid Dispersions Revealed by Solid-State 2H NMR Spectroscopy, Small Angle X-ray Scattering, and Molecular Theory. Biophysical Journal. 2009 November 15; 97(10): 2700-2709.

Xu F, Zhang H, IIavsky J, Stanciu L, Ho D, **Justice MJ**, Petrache HI, Xie J. Investigation of a catalyst ink dispersion using both ultra-small-angle X-ray scattering and cryogenic TEM. Langmuir. 2010 Dec 21;26(24): 19199-19208.

Mallikarjunaiah KJ, Leftin A, Kinnun JJ, **Justice MJ**, Rogozea A, Petrache HI, Brown MF. Solid-State ^{2}H NMR Shows Equivalence of Dehydration and Osmotic Pressures in Lipid Membrane Deformation**.** Biopysical Journal. 2011 January 5; 100(1): 98-107.

Schweitzer KS, Hatoum H, Brown MB, Gupta M, **Justice MJ**, Beteck B, Van Demark M, Gu Y, Presson RG Jr, Hubbard WC, Petrache I. 2011. Mechanisms of Lung Endothelial Barrier Disruption Induced by Cigarette Smoke: Role of Oxidative Stress and Ceramides. American Journal of Physiology - Lung Cellular and Molecular Physiology. 2011 December; 301(6): L836-L846.

Lahm T, Albrecht M, Fisher A, Selej M, Patel N, **Justice MJ**, Brown M, Van Demark M, Trulock K, Reddy J, Presson R, Petrache I. 17-beta Estradiol Attenuates Hypoxic Pulmonary Hypertension via Estrogen Receptor-Mediated Effects. American Journal of Respiratory and Critical Care Medicine. 2012 May 1;85(9); 965-980.

Green L, Petrusca DN, Rajashekhar G, Gianaris T, Schweitzer K, Wang L, **Justice MJ**, Petrache I, Clauss M. Cigarette Smoke-Induced CXCR3 Receptor Upregulation Mediates Endothelial Apoptosis. 2012. American Journal of Respiratory Cell and Molecular Biology. Published on August 30, 2012 as doi:10.1165/rcmb.2012-0132OC.

Bardita C, Predescu D, **Justice MJ**, Petrache I, Predescu S. In vivo knockdown of intersectin-1s alters endothelial cell phenotype and causes microvascular remodeling in the mouse lungs. Apoptosis. Published on January 18, 2013 as doi: 10.1007/s10495-012-0762-x.

Petrache I, Kamocki K, Poirier C, Pewzner-Jung Y, Laviad E L, Schweitzer KS, Van Demark M, **Justice MJ**, Hubbard WC, and Futerman AH. Ceramide synthases expression and role of ceramide synthase-2 in the lung: insight from human lung cells and mouse models. PloS One. 2013. Accepted.

Petrusca DN, Van Demark M, Gu Y, **Justice MJ**, Rogozea A, Hubbard WC, Petrache I. Smoking Exposure Induces Human Lung Endothelial Cells Adaptation to Apoptotic Stress. American Journal of Respiratory Cell and Molecular Biology. 2013.

Justice MJ, Petrusca DN, Wassal S, Petrache I, Petrache HI. Effects of Lipid Integrations on Model Membrane Engulfment by Macrophages. *in review (Biophysical Journal)*.

INVITED TALKS AND PRESENTATIONS

Matthew J. Justice, Horia I. Petrache, Measurements of Electrostatic Interactions between Charged Membranes, Indiana Academy of Science, University of Evansville, 2008.

Matthew J. Justice, Horia I. Petrache, X-ray Measurements of Multilamellar Lipid Structures, IUPUI Biomembrane Sciences Center, 2008.

Matthew J. Justice, Horia I. Petrache, Ceramide inhibits apoptotic cell clearance by affecting cell membrane fusion**,** IUPUI Biomembrane Sciences Center, 2009.

Matthew J. Justice, Effects of lipid interactions on model vesicle engulfment by alveolar macrophages. International Ceramide Conference. Montauk, NY. 2013

POSTER PRESENTATIONS

Matthew J. Justice, Carina Poltera, Horia I. Petrache, Electrostatic interactions in membrane systems. Symposium on Frontiers in Biological Membranes, Purdue University, West Lafayette, 2008.

Matthew J. Justice, Carina M. Poltera, Horia I. Petrache, Measurements of Electrostatic Interactions between Charged Membranes. 53rd Biophysical Society Meeting. Boston. Biophysical Journal 96(3) pp. 459a, 2009.

Matthew J. Justice, Adriana L. Rogozea, Daniela N. Petrusca, Irina Petrache, Stephen R. Wassall, Horia I. Petrache, The Effect of Ceramide on Model Membranes and Apoptotic Cells Determined by X-Ray Scattering, Solid State NMR, and Flow Cytometry. 54th Biophysical Society Meeting. San Francisco. Biophysical Journal 98(3) pp. 465a-466a, 2010.

Matthew J. Justice, Adriana L. Rogozea, Daniela N. Petrusca, Kelly Schweitzer, Irina Petrache, Stephen R. Wassall, Horia I. Petrache. The Role of Ceramide in the Clearence of Apoptotic Cells. 55th Biophysical Society Meeting. Baltimore. Biophysical Journal 100(3) pp. 409a, 2011.

Matthew J. Justice, Daniela N. Petrusca, Justin Williams, Kelly S. Schweitzer, Irina Petrache, Stephen R. Wassall, Horia I. Petrache. Engulfment of Model Membranes by Alveolar Macrophages. 56th Biophysical Society Meeting. San Diego. Biophysical Journal 102(3) pp. 502a, 2012.

Matthew J. Justice, K. Schweitzer, D.N. Petrusca, I. Petrache. Control of Cigarette Smoke-Induced Apoptosis or Autophagy by Acid Sphingomyelinase. American Thoracic Society International Conference. Philadelphia. American Journal of Respiratory and Critical Care Medicine 187;2013:A5180, 2013.

PUBLISHED ABSTRACTS

Avigdor Leftin, **Matthew J. Justice**, Jacob G. Kinnun, Horia I. Petrache, Michael F. Brown, Structural and Dynamic Markers of Membrane Osmotic Stress From X-Ray Scattering and Solid-State 2H NMR. 53rd Biophysical Society Meeting. Boston. Biophysical Journal 96(3) pp. 356a, 2009.

Andrey Struts, David P. Holland, Gabriel Longo, **Matthew J. Justice**, Igal Szleifer, Avigdor Leftin, Horia I. Petrache, Michael F. Brown, David H. Thompson, Phase Separation in Binary Mixtures of Bipolar and Monopolar Lipid Dispersions Revealed by Solid-State 2H NMR Spectroscopy and Small Angle X-ray Scattering. 53rd Biophysical Society Meeting. Boston. Biophysical Journal 96(3) pp. 355a, 2009.

Adriana L. Rogozea, **Matthew J. Justice**, Horia I. Petrache, Molecular Hydration Investigated using Extended Membrane Surfaces. 54th Biophysical Society Meeting. San Francisco. Biophysical Journal 98(3) pp. 689a, 2010.

K.J. Mallikarjunaiah, Avigdor Leftin, Jacob J. Kinnun, **Matthew J. Justice**, Adriana L. Rogozea, Horia I. Petrache, Michael F. Brown, Osmotic Membrane Deformation Revealed by Solid-State 2H NMR and Small-Angle X-Ray Scattering. 54th Biophysical Society Meeting. San Francisco. Biophysical Journal 98(3) pp. 282a, 2010.

Megan M. Koerner, **Matthew J. Justice**, Bruce D. Ray, Horia I. Petrache, Buffer Properties Revealed with Model Lipid Membranes. 54th Biophysical Society Meeting. San Francisco. Biophysical Journal 98(3) pp. 273a-274a, 2010.

K.J. Mallikarjunaiah, Jacob J. Kinnun, Avigdor Leftin, Luis A. Palacio, **Matthew J. Justice**, Horia I. Petrache, Michael F. Brown. Area Deformation of Membranes from the Perspective of ^{2}H NMR and X-ray Scattering. 55th Biophysical Society Meeting. Baltimore. *Biophysical Journal*100(3) pp. 173a, 2011.

Kelly S. Schweitzer, **Matthew J. Justice**, Margie Albrecht, Mary Van Demark, Yuan Gu, Yong Gao, Krzysztof Kamocki, Robert Bittman, Irina Petrache. Therapeutic Potential of FTY720-Analogs in Cigarette-Smoke Induced Lung Injury that is Dependent Upon

Sphingosine-1 Phosphate Receptor-1, S1PR1. American Thoracic Society International Conference. San Francisco. 2012.

Daniela N. Petrusca, **Matthew J. Justice**, Robert Bittman, Kelly Schweitzer, Walter C. Hubbard, Homer L. Twigg, and Irina Petrache. FTY720 Analogs Improve Alveolar Macrophages Efferocytosis During Cigarette Smoking. American Thoracic Society International Conference. San Francisco. 2012.

Matthias Clauss, Gangaraju Rajashekhar, Robert Voswinckel, Kelly Schweitzer, **Matthew J. Justice**, and Irina Petrache. Involvement of Monocytes in EMAP II Induced Alveolar Airspace Enlargement. American Thoracic Society International Conference. San Francisco. 2012.

Kelly Schweitzer, **Matthew J. Justice**, Margie Albrecht, Mary Van Demark, Jordan Wood, Krzysztof Kamocki, Mariam Qureshi, Zorina Galis, Irina Petrache. Role Of EMMPRIN In Cigarette-Smoke Induced Emphysema. American Thoracic Society International Conference. Philadelphia. 2013.

Karina A. Serban, Daniela N. Petrusca, Angelia D. Lockett, **Matthew J. Justice**, Irina Petrache. Alpha 1 Antitrypsin Effect On Alveolar Macrophages Engulfment Of Apoptotic And Phagocytic Targets. American Thoracic Society International Conference. Philadelphia. 2013.

Christophe Poirier, **Matthew J. Justice**, Mary Van Demark, Yuan Gu, Walter Hubbard, Irina Petrache. The Importance Of Constitutive Acid Sphingomyelinase (aSMase) For The Maintenance Of Lung Function During Development And Exposure To Cigarette Smoke (CS). American Thoracic Society International Conference. Philadelphia. 2013.

Matthias Clauss, Gangaraju Rajashekhar, Robert Voswinckel, Kelly Schweitzer, **Matthew J. Justice**, Irina Petrache. Involvement Of Monocytes In EMAP II-Induced Alveolar Airspace Enlargement. American Thoracic Society International Conference. Philadelphia. 2013.